LIMITING ACTIVITY COEFFICIENTS AND GAS–LIQUID PARTITION COEFFICIENTS OF ALKYLBENZENES IN HYDRO–ORGANIC SOLVENTS

WON JO CHEONG and PETER W. CARR*

Department of Chemistry, Smith Hall, University of Minnesota, 207 Pleasant Street S.E., Minneapolis, MN 55455 (U.S.A.)

(First received May 3rd, 1989; revised manuscript received August 18th, 1989)

SUMMARY

The limiting activity coefficients and gas–liquid partition coefficients of a series of n-alkylbenzenes (benzene to n-butylbenzene), cumene and *tert.*-butylbenzene have been measured in mixtures of water with methanol, acetonitrile, isopropanol and tetrahydrofuran over a wide range in composition. The reproducibility of the measured data for 3–4 replicate runs was generally better than 5%. Activity coefficients have been studied as a function of volume fraction, π^* (Kamlet–Taft solvent polarity/polarizability scale), E_T (solvent polarity scale based on Reichardt's betaine) and surface tension. None of these solvent properties gives a universal curve for the different solvent systems. The overall free energy of the solution process was computed using the activity coefficient and the free energy of cavity formation was computed via the Sinanoglu–Reiss–Moura Ramos solvophobic model. The individual free energy terms were examined in terms of their dependence on solute size and solvent composition. The results were generally consistent with chemical expectations. The UNIFAC model of activity coefficient was examined. The predicted values of the limiting activity coefficients for the non-polar solutes in these aqueous solvents were disappointing. We suspect that the UNIFAC parameters needed to predict these systems are based on poor data.

INTRODUCTION

Activity coefficients and partition coefficients of prototypical non-polar solutes such as alkylbenzenes in methanol–water, acetonitrile–water, isopropanol–water and tetrahydrofuran–water mixtures are very important in many areas. For example, in reversed-phase liquid chromatography (RPLC) such data can be used to explore the effect of the mobile phase on solute retention and to examine the mechanism of retention[1,2]. They can also be used to study the solution thermodynamics of aqueous mixtures. Predictive models for activity coefficients such as UNIFAC[3] and ASOG (analytical solution of groups)[4] are not successful for estimating properties of non-polar solutes in aqueous solvents[5]. This is due not only to the severe non-ideality of aqueous solvent systems but also to the scarcity of reliable data from which the

model parameters can be derived[6]. Difficulties in measuring limiting activity coefficients of non-polar solutes in very polar solvents are due to the very limited range of validity of the Henry's law region and the low solubility of non-polar substances in these systems. For the above reasons activity coefficients (and gas–liquid partition coefficients) of a set of alkylbenzenes in common RPLC solvents over a wide range of solvent composition have not been reported. It should be noted, however, that Tucker *et al.*[7] obtained very accurate measurement of the activity coefficient of benzene in pure water using a highly sensitive vapor pressure apparatus.

Headspace gas chromatography (HSGC) was used in this work to measure the activity coefficients. The advantages of the HSGC method over other approaches have been discussed elsewhere[8,9]. The main advantages of HSGC are its versatility and speed in acquiring a large amount of data[8]. Applications of activity coefficients to the study of liquid chromatography can be found elsewhere[10]. In this work data are reported and analyzed in terms of solution thermodynamics. In addition the utility of the UNIFAC method for predicting properties of the alkylbenzenes in hydro–organic mixtures and its limitations are examined.

EXPERIMENTAL

HPLC-grade water, methanol, acetonitrile, isopropanol and tetrahydrofuran (purity 99.9%, Fisher Scientific) were used throughout. The alkylbenzenes (purity greater than 99%) were used without further purification. Details of the HSGC system used in this work have been presented elsewhere at great length[9,11]. In essence a known amount of solute is delivered to a closed cell, allowed to equilibrate between the liquid and gas phase and then the gas phase is sampled. The composition of the solvent is varied by adding a known amount of water. Thus we can immediately compute the gas–liquid partition coefficient from the experimental data. By use of the well known relationship between the partition coefficient and the infinite dilution activity coefficient we can compute the activity coefficient in the liquid phase. In all the data reported here the activity coefficients were based on Raoult's law as the standard state, thus the activity coefficients approach unity as the mole fraction of the test solute approaches unity.

Actually the calculations are slightly more complex than implied above. Since we add a known amount of solute to the cell and in the systems studied here the solute has a great tendency to transfer into the gas phase a significant fraction of the solute added is actually present in the gas phase. Thus in calculating activity coefficients, the liquid phase concentration was computed based on the total amount of solute added, the total volume of liquid and gas phases and the measured amount of solute in the gas phase. In the worst case only 5% of the solute was present in the gas phase. Since some gas was removed upon sampling the cell the total amount of solute was depleted. In the worst case the total amount of sample removed from the cell during the course of the entire set of runs was less than 2%. Computer programs for the implementation of all calculations are available from the corresponding author.

The experimental procedure described in refs. 9 and 11 was modified slightly to overcome the very low solute solubilities in aqueous solvents. Since the non-polar solutes dissolved very slowly in water-rich solvents, they were predissolved in the organic solvent of interest such that the total volume fraction was about 10%.

A 10–30-ml volume of an organic solvent was added to a thermostated cell maintained at $25 \pm 0.005°C$. A 50–500-μl volume of the solute mixture in the solvent of interest was transferred to the cell via a gas-tight syringe. After 60 min of equilibration three replicate GC analyses of the headspace vapor above the solvent were performed via our computer controlled headspace gas chromatograph. Aliquots of water (typically 1–3 ml) were added via a computer-controlled buret. Water was added stepwise to vary the solvent composition. The composition of the mixture was varied, in different runs, from the pure solvent to 0.4–0.7 volume fraction water. The final solvent composition depended upon the volume of the organic solvent initially present in the cell. The volume fraction of organic cosolvent was taken as the volume of the organic solvent divided by the sum of the volumes of water and organic solvent before mixing. The solute concentration in the gas phase was measured by sampling the headspace at each composition. Three replicate analyses of the headspace were run subsequent to an hour of equilibration. Three to four separate runs with different amounts (5–50 μl) of the solute mixture were carried out to obtain data at different solute concentrations and to insure that we were working in the Henry's law region. For example, the initial solute mole fractions were about 10^{-4} in one methanol–water run and 10^{-5} in a second run. The solute mole fractions ranged from 10^{-6} to 10^{-4} depending upon the solvent system. In addition, solute activity coefficients in the pure organic solvents (methanol, acetonitrile, isopropanol and tetrahydrofuran) were also measured by our usual procedure[11] by adding the solute mixture stepwise and thereby collecting data at a series of solute concentrations.

An activity coefficient standard solution (hereafter referred to as the ACSS) was prepared in isopropanol and used to check the system. The solute activity coefficients in the ACSS were constant over a long period of time provided that the system was working properly. The solute concentration of the ACSS (0.005–0.01 mole fraction) was much higher than the solute concentration in the thermostated cell (10^{-6}–10^{-4} mole fraction). The sole purpose of the ACSS was to check the reproducibility of the system and therefore the solute concentration in the ACSS need not be in the Henry's law region. Consequently the gas phase solute concentration of the ACSS was intentionally made much higher than that in the sample cell. A slight solute condensation–adsorption effect in the gas transfer system may be negligible for the ACSS but can be very significant for the sample in the cell. Therefore it was necessary to periodically run a sample in a reference solvent to check whether the transfer system was free of non-volatile contaminants. Methanol was used as the reference solvent.

RESULTS AND DISCUSSION

All of the hundreds of activity coefficients (γ) and gas–liquid partition coefficients are available upon request. The set of data provided in the appendix are given for the convenience of the interested reader.

The activity coefficient of benzene in the tetrahydrofuran–water system could not be measured because of overlap of the benzene peak with the solvent peak. The reproducibility of three replicate analyses as well as the difference between the area and height results were examined for each data point. If either was worse than 5%, the data were excluded. This happened most commonly with the data at greater than 0.9 volume fraction of the organic cosolvent due to the small size of the solute peak and

overlap of the solute peak with the tail of the solvent peak. The reproducibility was also checked between runs. For example the reproducibility of activity coefficients of n-butylbenzene in the methanol–water mixtures for four different runs is shown in Fig. 1. Each symbol denotes a different run. In the course of comparing batch runs some evident outliers were excluded. Over the course of weeks impurities can be formed or trapped in the gas transfer system and they may overlap with a solute peak. This was sometimes observed for ethylbenzene and propylbenzene. Such data were excluded.
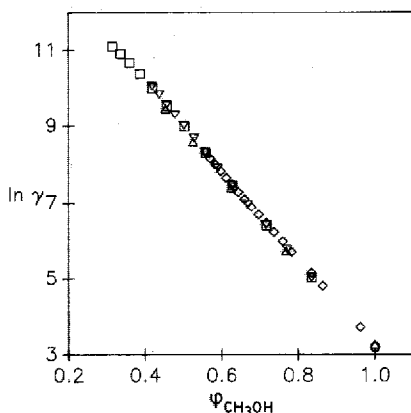

Fig. 1. Reproducibility of the activity coefficients of n-butylbenzene in methanol–water mixtures for four batch runs. Each symbol denotes a batch run. Initial solute mole fractions: $\triangle = 1.08 \cdot 10^{-4}$; $\square = 2.83 \cdot 10^{-5}$; $\nabla = 1.26 \cdot 10^{-5}$; $\diamond = 1.78 \cdot 10^{-4}$.

In order to compare the reproducibility of the data from run to run the γ^∞ were fitted to various approximating functions. For the methanol–water system $\ln \gamma^\infty$ can be rather accurately represented as a linear function of volume fraction (see Tables I and II). As summarized in Table I the average standard deviation of the fit, when all of the various runs in the methanol systems were fit simultaneously, varied from 0.03 for benzene to 0.06 for n-butylbenzene. Given the enormous range in $\ln \gamma^\infty$ observed we felt that this precision was adequate for our purposes.

The data for other solvent systems were fit to two distinct models as follows:

$$\ln \gamma^\infty = A + B_1 \varphi + B_2 \varphi^2 + B_3 \varphi^3 \tag{1}$$

$$\ln \gamma^\infty = (a + b \varphi)/(1 + c \varphi) \tag{2}$$

where φ is the volume fraction of the organic cosolvent. Eqn. 2 (a Pade approximant) is known to be a powerful method for fitting smoothly varying monotonic curves. The polynomial curve obtained by fitting to eqn. 1 was, however, more precise than that obtained by eqn. 2 for the data of this study. The average standard deviations of the two methods are compared in Table I. The regression results of the polynomial curve fitting are given in Table II.

TABLE I

REPRODUCIBILITY OF MEASUREMENT AS ASSESSED BY CURVE FITTING

All the data of different batch runs were simultaneously fitted to a universal curve.

System	φ	Solute	Average S.D. in $\ln \gamma^{\infty}$	
			Based on eqn. 1	Based on eqn. 2
Methanol[a]	$0.3147 \leqslant \varphi \leqslant 1.0$	Benzene (B)	0.03	—[b]
		Toluene (T)	0.03	—
		Ethylbenzene (EB)	0.04	—
		Propylbenzene (PB)	0.05	—
		Butylbenzene (BB)	0.06	—
		Cumene (C)	0.05	—
		tert.-Butylbenzene (TB)	0.05	—
Acetonitrile	$0.2963 \leqslant \varphi \leqslant 1.0$	Benzene	0.02	0.05
		Toluene	0.03	0.07
		Ethylbenzene	0.03	0.09
		Propylbenzene	0.06	0.10
		Butylbenzene	0.02	0.12
		Cumene	0.03	0.10
		tert.-Butylbenzene	0.03	0.11
Isopropanol	$0.2951 \leqslant \varphi \leqslant 1.0$	Benzene	0.02	0.04
		Toluene	0.02	0.06
		Ethylbenzene	0.03	0.07
		Propylbenzene	0.04	0.08
		Butylbenzene	0.05	0.10
		Cumene	0.04	0.08
		tert.-Butylbenzene	0.04	0.09
Tetrahydrofuran	$0.3654 \leqslant \varphi \leqslant 1.0$	Toluene	0.02	0.05
		Ethylbenzene	0.02	0.07
		Propylbenzene	0.03	0.09
		Butylbenzene	0.05	0.11
		Cumene	0.03	0.08
		tert.-Butylbenzene	0.03	0.09

[a] Fitted to a first order linear function.
[b] Regressions based on eqn. 2 were not done because a straight line fits the data.

We also assessed higher order polynomials of the form of eqn. 1 but additional terms were not needed. Again we note that based on eqn. 1, when all of the data in several different runs were simultaneously fit, the average deviation of the fit never exceeded 0.06 and was generally 0.02–0.03. We deem this precision to be acceptable for present purposes.

The data for each individual run, representing a different solute concentration, were also fitted to a best-fit polynomial function (first, second or third order according to the solvent composition range) in order to compute interpolated values at selected solvent compositions and to compare the data from different runs. The interpolation was limited to the composition range for which each data set was collected. Thus the computed $\ln \gamma^{\infty}$ of n-butylbenzene, for example, was plotted against the volume of solute mixture added to the cell (Fig. 2). The γ^{∞} values of different batch runs are

TABLE II

THE REGRESSION RESULTS FOR FITTING ln γ^{∞} TO A POLYNOMIAL

All data fit to eqn. 1. The average standard deviation and the composition range are summarized in Table I.

System	Solute[a]	$A \pm$ S.D.	$B_1 \pm$ S.D.	$B_2 \pm$ S.D.	$B_3 \pm$ S.D.	r	n
Methanol–water	B	9.00 ± 0.02	-7.06 ± 0.02	$-$[b]	$-$[b]	0.99969	55
	T	10.33 ± 0.02	-8.04 ± 0.02	$-$	$-$	0.99977	54
	EB	11.73 ± 0.02	-9.17 ± 0.03	$-$	$-$	0.99979	34
	PB	13.24 ± 0.03	-10.47 ± 0.04	$-$	$-$	0.99959	51
	BB	14.82 ± 0.03	-11.68 ± 0.05	$-$	$-$	0.99955	48
	C	12.86 ± 0.03	-10.08 ± 0.04	$-$	$-$	0.99957	52
	TB	13.82 ± 0.03	-10.95 ± 0.04	$-$	$-$	0.99961	51
Acetonitrile–water	B	9.55 ± 0.87	-16.11 ± 0.44	13.46 ± 0.71	-5.81 ± 0.36	0.99993	39
	T	11.32 ± 0.13	-20.29 ± 0.66	18.46 ± 1.06	-8.04 ± 0.54	0.99986	40
	EB	13.22 ± 0.14	-25.09 ± 0.71	24.38 ± 1.16	-10.75 ± 0.60	0.99987	39
	PB	14.78 ± 0.21	-28.01 ± 1.10	27.52 ± 1.79	-12.24 ± 0.93	0.99977	35
	BB	16.92 ± 0.13	-33.92 ± 0.68	35.10 ± 1.10	-15.66 ± 0.57	0.99992	38
	C	14.65 ± 0.15	-28.54 ± 0.76	28.38 ± 1.24	-12.51 ± 0.64	0.99988	39
	TB	15.83 ± 0.15	-31.56 ± 0.80	32.09 ± 1.29	-14.23 ± 0.67	0.99988	39
Isopropanol–water	B	10.58 ± 0.08	-18.82 ± 0.42	16.71 ± 0.67	-6.99 ± 0.33	0.99993	42
	T	12.69 ± 0.11	-25.24 ± 0.56	24.68 ± 0.89	-10.50 ± 0.45	0.99990	41
	EB	14.81 ± 0.15	-31.80 ± 0.75	33.10 ± 1.21	-14.31 ± 0.62	0.99986	40
	PB	17.08 ± 0.20	-39.35 ± 1.02	43.21 ± 1.66	-19.05 ± 0.86	0.99979	38
	BB	18.98 ± 0.28	-45.02 ± 1.43	50.44 ± 2.32	-22.31 ± 1.20	0.99966	37
	C	16.48 ± 0.20	-37.11 ± 1.00	39.81 ± 1.60	-17.29 ± 0.82	0.99979	40
	TB	17.94 ± 0.22	-42.06 ± 1.15	46.61 ± 1.88	-20.55 ± 0.97	0.99975	38
Tetrahydrofuran–water	T	12.04 ± 0.20	-26.76 ± 0.93	25.55 ± 1.41	-11.04 ± 0.69	0.99991	36
	EB	13.91 ± 0.21	-32.54 ± 1.00	32.89 ± 1.52	-14.39 ± 0.74	0.99991	36
	PB	15.61 ± 0.32	-37.61 ± 1.52	39.07 ± 2.32	-17.21 ± 1.13	0.99983	36
	BB	17.36 ± 0.50	-43.14 ± 2.41	45.84 ± 3.67	-20.22 ± 1.81	0.99960	34
	C	15.24 ± 0.25	-36.48 ± 1.20	37.60 ± 1.82	-16.51 ± 0.89	0.99989	36
	TB	16.42 ± 0.32	-40.25 ± 1.55	42.37 ± 2.36	-18.70 ± 1.16	0.99983	35

[a] Solute symbols defined in Table I.
[b] Coefficient not needed to fit the data.

consistent as shown in Fig. 2. In general the differences for separate batch runs, which span a ten-fold range in solute concentration, are less than 10% (mostly 5%). Because of the very low solubility of non-polar solutes in predominantly aqueous solvents, the volume fraction of water was limited to a maximum of 0.7. It should be noted that the error in the measured activity coefficient of solutes with high boiling point such as n-butylbenzene could be 10% or somewhat greater due to condensation–adsorption of the solute on the surface of the vapor transfer system. The temperature of the transfer system was always 170–175°C in this work while the boiling point of n-butylbenzene is 180°C.

The logarithms of the solute activity coefficients are plotted against volume fraction of the organic cosolvent. In Fig. 3 the raw data for all the batch runs were simultaneously plotted. The rather linear plots observed for the methanol–water system may be due to the similarity in the structure and polarity of water and
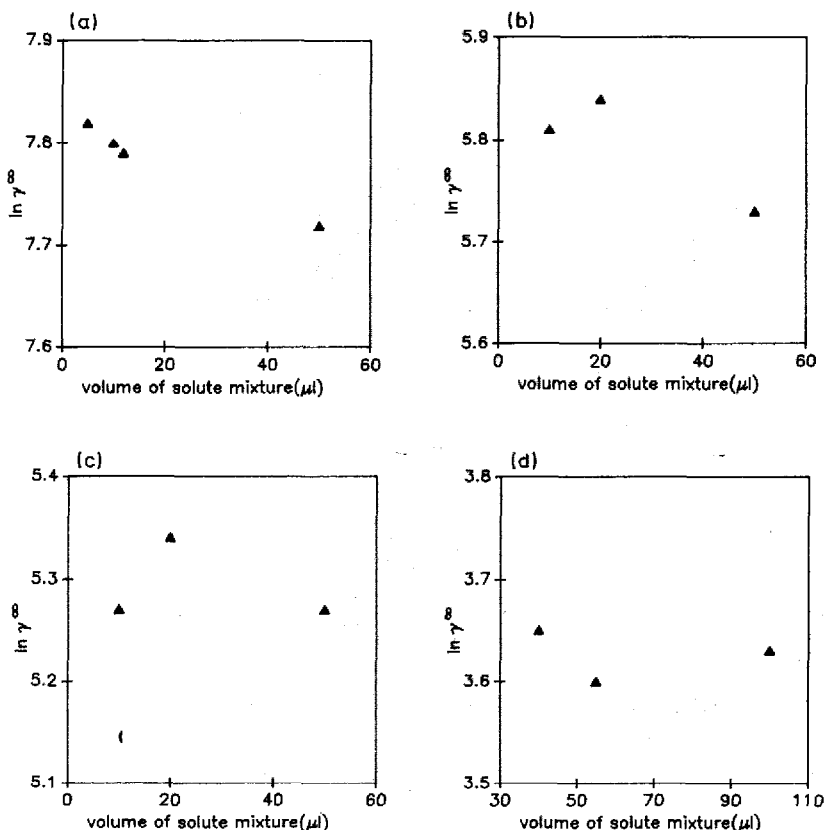
Fig. 2. ln γ^∞ vs. volume of the solute mixture added to the cell. Volume fraction of organic cosolvent: 0.6. (a) Methanol–water system; (b) acetonitrile–water system; (c) isopropanol–water system; (d) tetrahydrofuran–water system.

methanol. The plots for the acetonitrile–water, isopropanol–water and tetrahydro-furan–water systems are all highly curved at lower φ. The results of the ACSS runs are shown in Table III. The reproducibility of the ACSS runs is generally better than 2% and better than 1% for solutes of low boiling point. The results of the reference solvent (methanol) runs are given in Table IV. The reproducibility is generally better than 3%.

Examination of the logarithm of the activity coefficient as a function of solvent properties
        In this work all activity coefficients are based on the use of Raoult's law. Thus $RT \ln \gamma^\infty$ (where R is the molar gas constant and T is temperature) is equivalent to the transfer free energy of 1 mole of solute from its pure state to a unit mole fraction solution of the solute acting as a hypothetically infinitely dilute solution. It includes solute–solvent interactions, solvent–solvent interactions (the cavity formation free energy) and solute–solute interactions in the standard state. For a single solute solvent-dependent variations in γ^∞ are not influenced by solute–solute interactions. It would be very helpful in understanding solute–solvent interactions if a universal
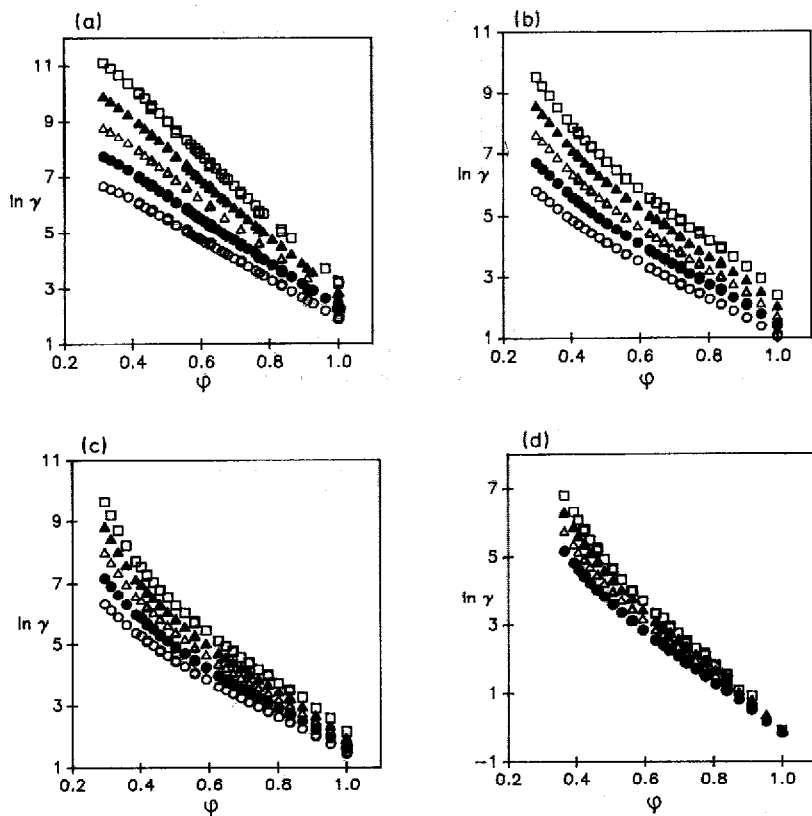
Fig. 3. The logarithm of activity coefficient *vs.* volume fraction of organic cosolvent. Symbols: ○ — benzene; ● = toluene; △ = ethylbenzene; ▲ = *n*-propylbenzene; □ = *n*-butylbenzene. (a) Methanol–water system; (b) acetonitrile–water system; (c) isopropanol–water system; (d) tetrahydrofuran–water system.

solvent property existed such that plots of γ^∞ *vs.* that property were to fall on a single universal curve regardless of the solvent. Such a property could exist only if the sum of solute–solvent and solvent–solvent interactions were proportional to the product of the solute and solvent properties. We plotted $\ln \gamma^\infty$ of toluene and *n*-butylbenzene with respect to various solvent properties such as φ, π^* (Kamlet–Taft solvent polarity/polarizability scale), E_T (solvent polarity scale based on Reichardt's betaine) and the surface tension (σ, see Figs. 4 and 5). None of these solvent properties resulted in a single universal curve for the four different solvent systems. In addition, trends in variation in γ^∞ *vs.* one solvent property are very different from that against another property. Such a universal solvent property is unlikely to exist since solute–solvent and solvent–solvent interactions are very complex. In contrast to the lack of universality between solvents, all of the non-polar solutes examined here behave similarly.

TABLE III

THE REPRODUCIBILITY OF ACTIVITY COEFFICIENTS IN ACTIVITY COEFFICIENT STANDARD SOLUTION

Run No.	Benzene	Toluene	Ethyl-benzene	Propyl-benzene	Butyl-benzene	Cumene	tert.-Butyl-benzene
1	3.70	4.40	5.28	6.21	7.77	5.82	6.58
2	3.74	4.43	5.31	6.30	7.97	5.88	6.65
3	3.69	4.40	5.31	6.19	7.70	5.77	6.51
4	3.73	4.45	5.31	6.20	7.36	5.80	6.48
5	3.73	4.47	5.36	6.28	7.57	5.86	6.53
6	3.76	4.51	5.39	6.27	7.64	5.88	6.55
7	3.70	4.40	5.29	6.20	7.70	5.79	6.48
8	3.73	4.45	5.31	6.14	7.43	5.75	6.32
Average	3.73	4.44	5.32	6.23	7.64	5.82	6.52
R.S.D. (%)[a]	0.50	0.89	0.72	0.97	2.61	0.90	1.51

[a] The relative standard deviation (100 × standard deviation/average).

Thermodynamics of gas–liquid equilibria

The standard transfer free energy of a solute from the gas phase to the liquid phase is related to the gas–liquid partition coefficient as follows:

$$\Delta G^0 = -RT \ln K = -RT \ln \frac{RT}{V_1 \, \gamma_2^\infty \, p_2^0} \tag{3}$$

where K is the gas–liquid partition coefficient, V_1 the molar volume of the solvent, γ_2^∞ the limiting activity coefficient of the solute, and p_2^0 the vapor pressure of the solute. The solute vapor pressure data were collected from the literature[12]. According to Ben-Naim and Marcus[13-15], the most appropriate concentration scale for gas–liquid equilibria is the number density (molar concentration) scale since the molar concentration based free energy of solution directly probes the difference in the energy of interaction of the solute with the solvent. The standard free energy is defined for the solute transfer from the ideal gas phase at 1 M concentration to the liquid phase at

TABLE IV

THE REPRODUCIBILITY OF ACTIVITY COEFFICIENTS IN METHANOL

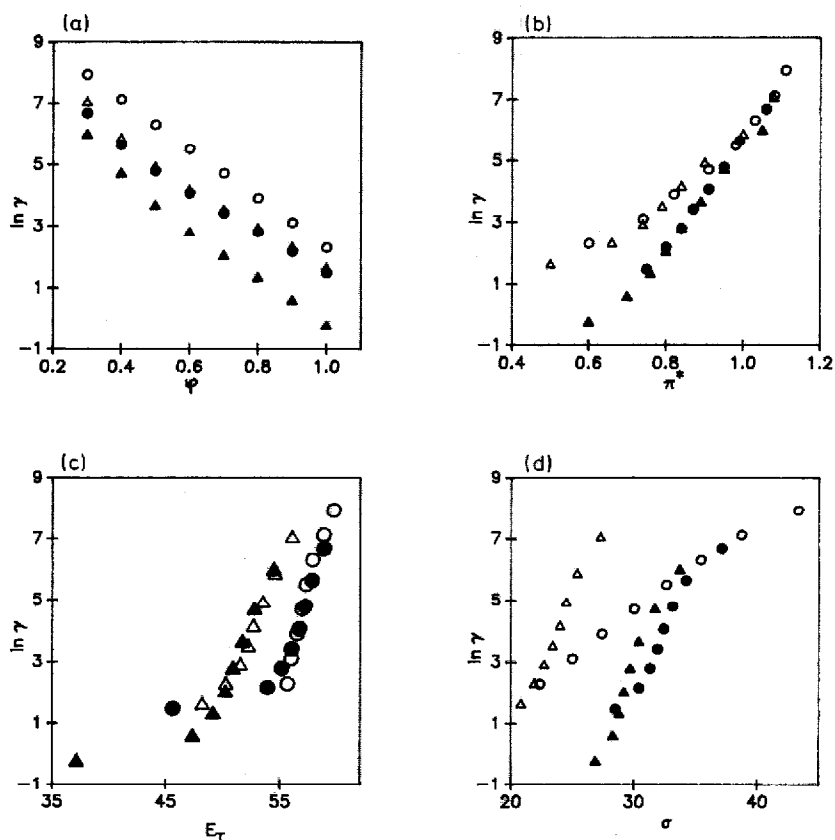| Run No.	Benzene	Toluene	Ethyl-benzene	Propyl-benzene	Butyl-benzene	Cumene	tert.-Butyl-benzene
1	6.75	9.57	13.0	17.1	24.1	15.6	18.9
2	6.82	9.67	13.3	17.5	24.4	15.9	19.3
3	6.82	9.53	12.9	16.9	23.9	15.5	18.9
Average	6.80	9.59	13.1	17.2	24.5	15.7	19.0
R.S.D. (%)	0.6	0.7	1.4	1.7	3.1	2.2	2.2

Fig. 4. The logarithm of activity coefficient of toluene *vs.* solvent properties. Symbols: ○ = methanol–water system; ● = acetonitrile–water system; △ = isopropanol–water system; ▲ = tetrahydrofuran–water system.

1 M concentration. The gas phase is assumed to be ideal. It is also assumed that there are only solute–solvent interactions in the liquid phase (no solute–solute interactions). The reference states (1 molar solute concentration) are clearly hypothetical.

The overall solution process can be described conceptually as taking place in two steps[16,17]. First a cavity of the correct size and shape to accept the solute is formed in the solvent. Second the cavity is filled with the solute and the solute is then allowed to interact with the solvent. The free energy of cavity formation is the work required to open a hole in the liquid phase. Solute molecules undergo various types of interactions with solvent molecules including: dispersive, dipole–dipole, dipole–induced dipole, and hydrogen bonding. Cavity terms are always positive (endoergic) while the interaction terms are always negative (exoergic). We can write:

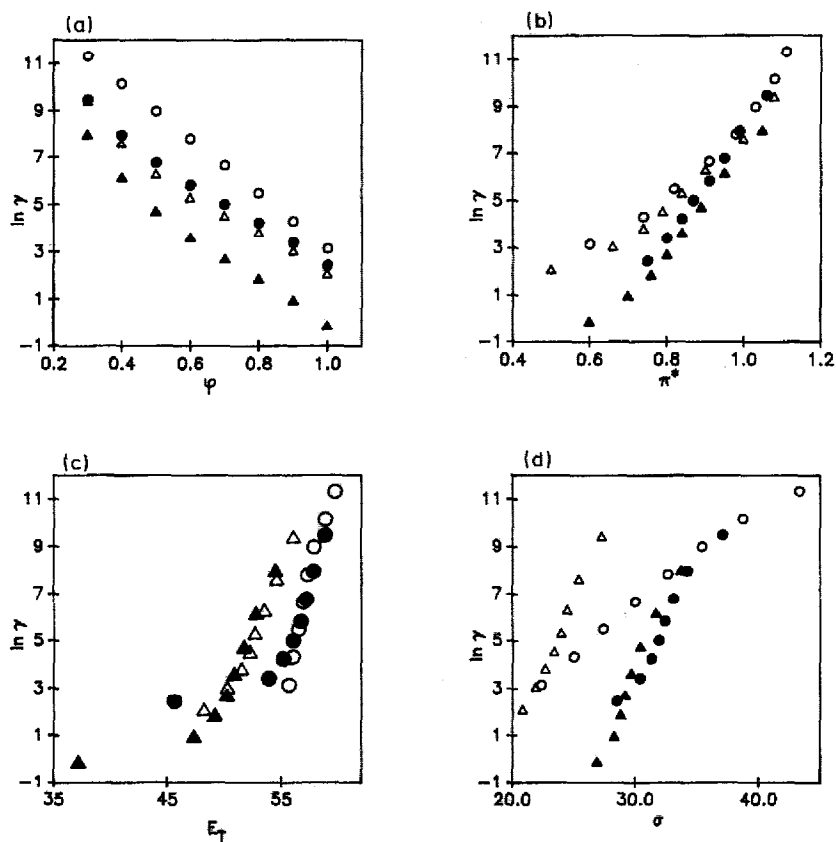$$\Delta G^0 = \Delta G_{tot} = \Delta G_{cav} + \Delta G_{int} \tag{4}$$

Fig. 5. The logarithm of activity coefficient of n-butylbenzene vs. solvent properties. Symbols: ○ = methanol–water system; ● = acetonitrile–water system; △ = isopropanol–water system; ▲ = tetrahydro-furan–water system.

where G_{tot} is the overall free energy, G_{cav} is the computed cavity formation free energy and G_{int} is the solvent–solute interaction free energy. We are not aware of any straightforward *a priori* methods for the direct calculation of solute–solvent interactions. On the other hand there are three common models for calculating the cavity formation free energies: Hildebrand *et al*.'s[16] solubility parameter theory, scaled particle theory[18,19], and the Sinanoglu–Reiss–Moura Ramos (SRMR) solvophobic models[20-22]. A comprehensive study of these models by Park[8] showed that the SRMR method gave the most reasonable cavity terms. Thus the SRMR method was used to estimate the cavity term in this study. The interaction term can be calculated by subtracting the cavity term from the measured overall free energy of transfer. The cavity term (cal/mol) is calculated by the SRMR method as follows[8,23]:

$$\Delta G_{cav} = H_{vap,1} + 9.761 \left[V_2^{2/3} - V_1^{2/3} \right] \sigma \qquad (5)$$

TABLE V

SOLVENT PROPERTIES

Solvent	H_{vap} (cal/mol)	V (ml/mol)	σ (dyne/cm)
Water	10 513.8	18.07	71.66
Methanol	8946	40.75	22.35
Acetonitrile	7873	52.87	28.49
Isopropanol	10 880	76.92	20.82
Tetrahydrofuran	7650	81.84	26.99

where $H_{vap,1}$ is the heat of vaporization of the solvent (cal/mol), V_2 and V_1 the solute and solvent molar volume (ml/mol), and σ the surface tension of the solvent (dyne/cm). It should be noted that the solvents used in this study are mixtures. We assumed a linear relationship for the dependence of the heat of vaporization and the molar volume on the mole fraction of the two components in the mixture. Thus the heat of
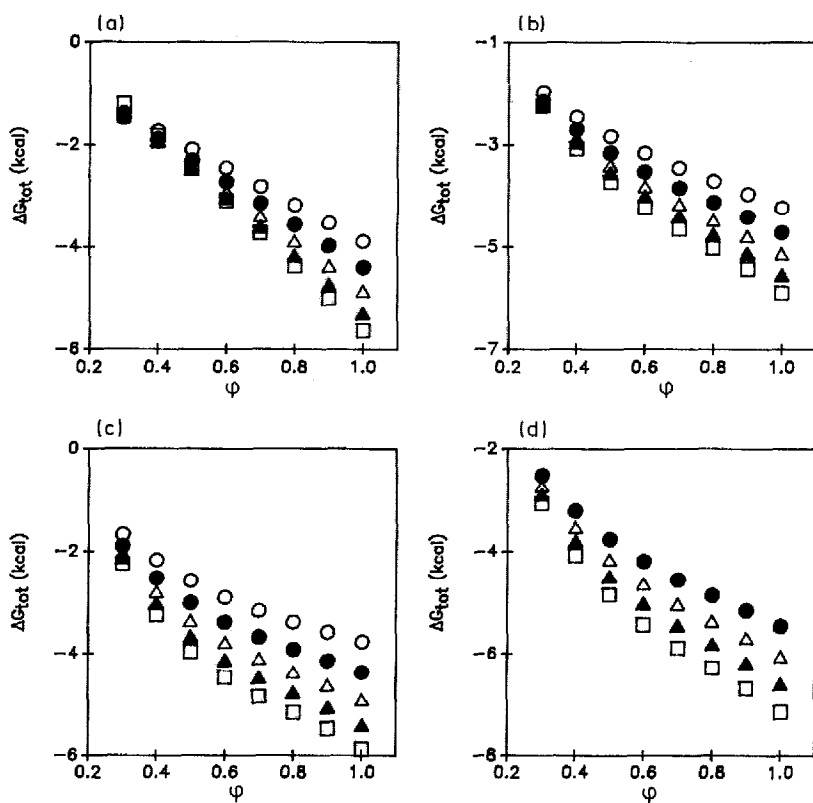

Fig. 6. The overall free energy of solution process vs. φ. Symbols: ○ = benzene; ● = toluene; △ = ethylbenzene; ▲ = n-propylbenzene; ☐ = n-butylbenzene. (a) Methanol–water system; (b) acetonitrile–water system; (c) isopropanol–water system; (d) tetrahydrofuran–water system.

vaporization and molar volume of the mixed solvents could be approximated using the properties of the pure organic solvents and water[12]. Surface tension data for aqueous mixtures were reported previously[24]. The relevant solvent properties are given in Table V.

The interaction free energy was computed by subtracting the cavity formation free energy from the measured overall free energy as follows:

$$\Delta G_{int} = \Delta G_{tot} - \Delta G_{cav}$$ (6)

ΔG_{tot}, ΔG_{cav} and ΔG_{int} values are plotted in Figs. 6, 7 and 8, respectively. The relative contributions of the cavity and interaction terms to the overall free energy are compared for ethylbenzene as a typical solute in Fig. 9. We will discuss the dependencies of the various free energy functions on solute size and solvent.

The dependence of the free energy terms on solute size are examined first. The magnitude of the exoergic cavity formation free energy increases with solute size (Fig. 7). This is consistent with the cavity formation concept. More energy is required to make a larger hole in the solvent. The energy of the computed solute–solvent interaction (based on eqn. 6) becomes more favorable as solute size increases (Fig. 8).
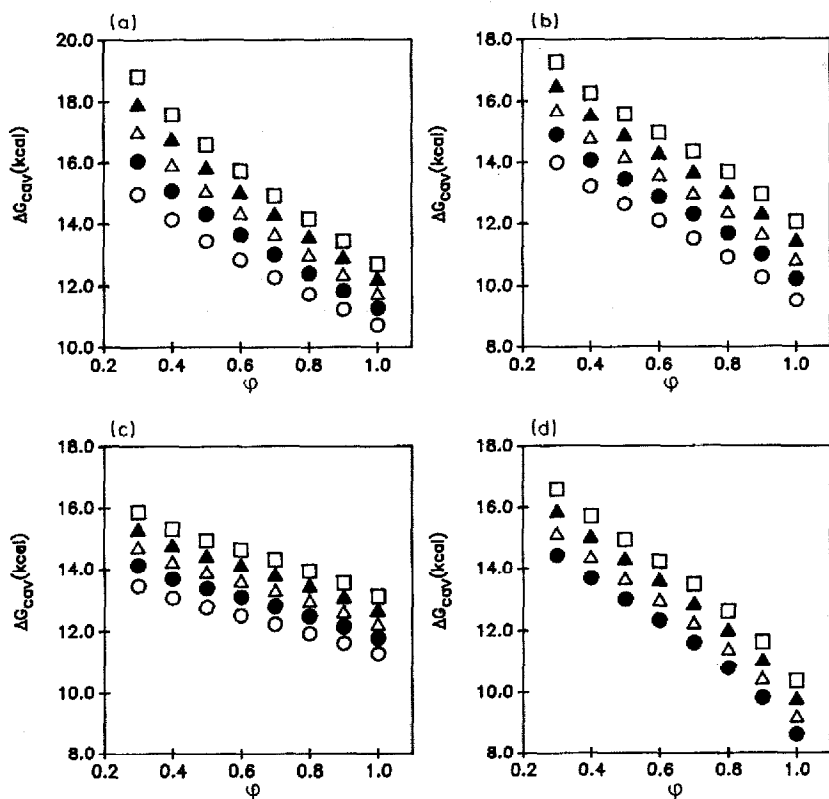

Fig. 7. The cavity formation free energy vs. φ. Symbols: $\bigcirc$ = benzene; $\bullet$ = toluene; $\triangle$ = ethylbenzene; $\blacktriangle$ = n-propylbenzene; $\square$ = n-butylbenzene. (a) Methanol–water system; (b) acetonitrile–water system; (c) isopropanol–water system; (d) tetrahydrofuran–water system.

Fig. 8. The solute–solvent interaction free energy *vs.* φ. Symbols: $\bigcirc$ = benzene; $\bullet$ = toluene; $\triangle$ = ethylbenzene; $\blacktriangle$ = *n*-propylbenzene; $\square$ = *n*-butylbenzene. (a) Methanol–water system; (b) acetonitrile–water system; (c) isopropanol–water system; (d) tetrahydrofuran–water system.
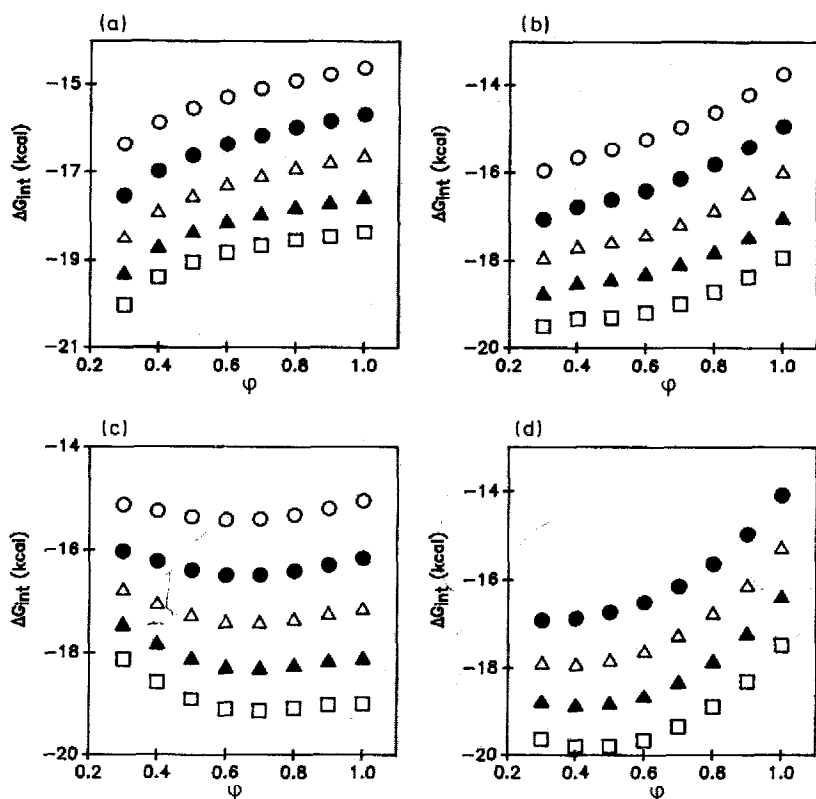
We believe that this is primarily due to an increase in the dispersive interactions between the solute and the solvent. Dispersive interactions are proportional to solute volume[25,26]. For larger solutes the cavity formation free energy is more endoergic and the interaction free energy is more exoergic.

The overall solution process is exoergic (negative ΔG_{tot} values) in all cases and becomes more exoergic as the solute size increases. This implies that the solute–solvent interaction increases more rapidly with solute size than does the cavity term. This can be explained as follows. The cavity formation process is closely related to the surface tension phenomenon. When a hole is formed in the solvent matrix the solvent molecules near the hole rearrange to minimize the energy disadvantage which arises from the loss of interaction with the molecules which were in the hole. Thus strongly interacting functional groups such as the hydroxyl group will orient themselves towards nearby polar groups in the bulk liquid[27]. When the hole is filled with a solute the surrounding molecules will be arranged to maximize the energy advantage. Thus the energy advantage for the solute–solvent interaction is greater than the energy disdadvantage for the loss of solvent–solvent interaction by the cavity formation
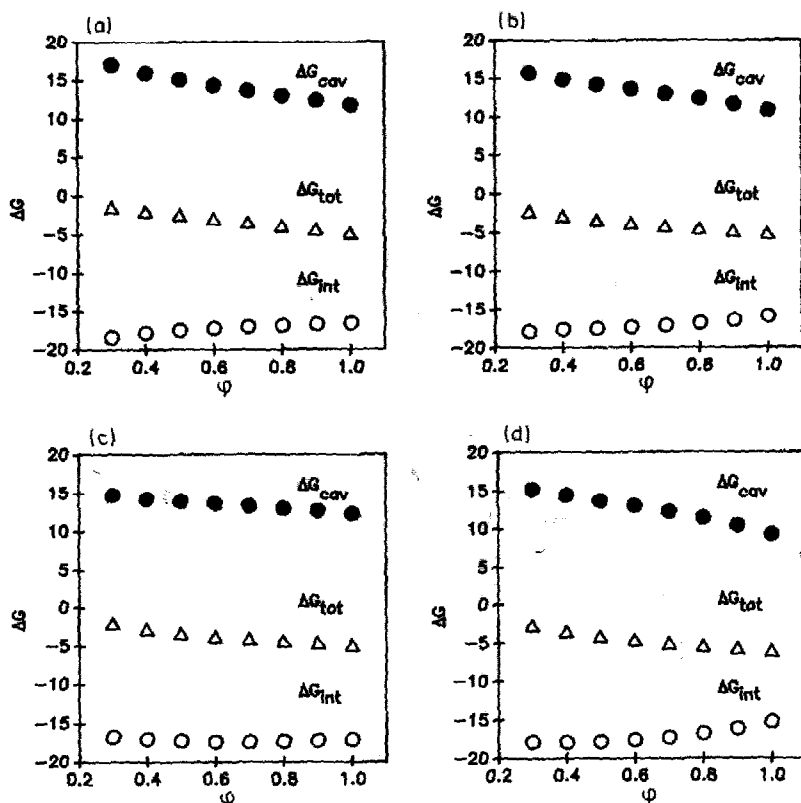
Fig. 9. Comparison of individual free energy terms for ethylbenzene as a test solute. Symbols: $\triangle$ = overall free energy; $\bullet$ = cavity formation free energy; $\bigcirc$ = interaction free energy. (a) Methanol–water system; (b) acetonitrile–water system; (c) isopropanol–water system; (d) tetrahydrofuran–water system.

process. Note that the solvent compositions considered in this study are from 0.3 to 1.0 volume fraction in the organic cosolvent.

The above argument may not be valid for pure water. For example, benzene is much more soluble in water than is n-butylbenzene[28]. Water is a highly structured medium and the surface tension of water is very high. Consequently in pure water the cavity term may be greater than the solute–solvent interaction term.

We believe that the enhanced cavity formation effect in water can be observed in plots of $\ln K$ for the gas-to-liquid transfer process vs. the solute carbon number (C_n) as a function of solvent composition (see Fig. 10). It is important to note that plots of $\ln K$ vs. carbon number are very analogous to plots of $\ln k'$, the capacity factor, vs. carbon number in gas chromatography. When interfacial adsorption is negligible in the gas chromatographic data $\ln k'$ and $\ln K$ should only differ by an additive constant related to the phase ratio. We are not aware of any set of k' data for an homologous series in which k' decreases as a CH_2 group is added thus the slope of these plots is invariably positive and they are in general good straight lines. Based on recent work of Schantz
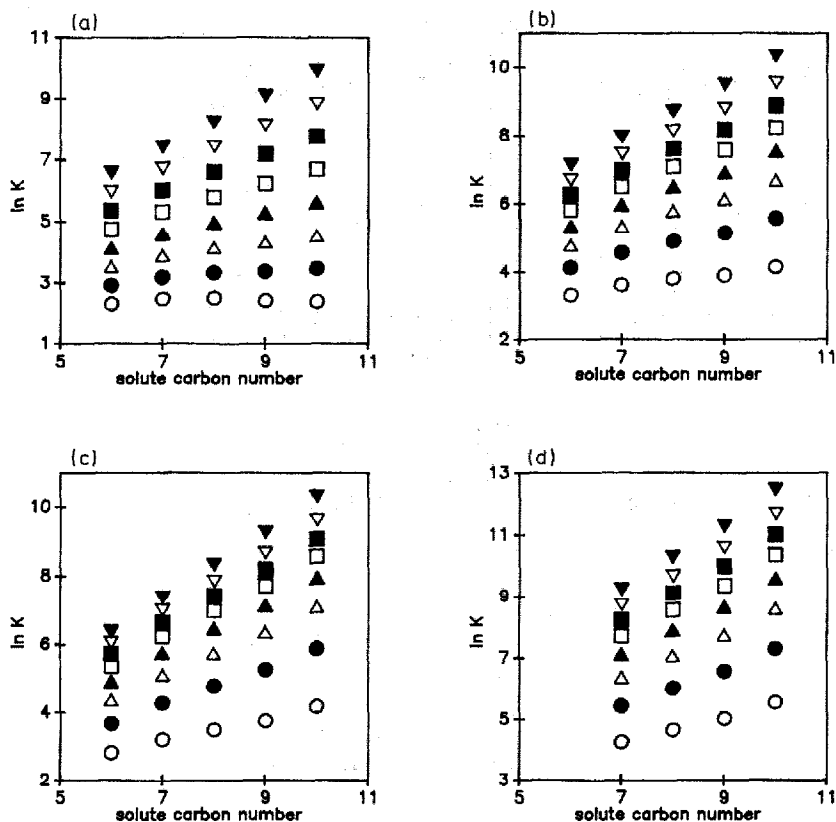
Fig. 10. ln K vs. solute carbon number. Volume fraction of organic cosolvent: $\bigcirc$ = 0.3; $\bullet$ = 0.4; $\triangle$ = 0.5; $\blacktriangle$ = 0.6; $\square$ = 0.7; $\blacksquare$ = 0.8; $\triangledown$ = 0.9; $\blacktriangledown$ = 1.0. (a) Methanol–water system; (b) acetonitrile–water system; (c) isopropanol–water system; (d) tetrahydrofuran–water system.

and Martire[29] for the alkylbenzenes in n-hexadecane at 25°C the following equation is obtained:

$$\ln K = -0.12\ (\pm 0.21) + 1.10\ (\pm 0.03)\ C_n \qquad (7)$$

$$\text{S.D.} = 0.08,\ r = 0.9992,\ n = 5$$

    Inspection of Fig. 10 shows that, in solvent mixtures containing a large fraction of organic solvent, plots of ln K vs. carbon number are straight and have high positive slopes. In contrast as the water content increases, partitioning from the gas into the liquid becomes less favorable, the slope decreases and for the highly aqueous systems the plots are no longer straight. Indeed for the methanol–water system at 30% methanol by volume the plot of ln K vs. carbon number has a shallow maximum and the K value for benzene and n-butylbenzene are nearly equal. This means that as the carbon number increases the solute partitioning changes in a direction initially

favoring the liquid phase but then begins to favor the gas phase. The above observations are consistent with the observation that the higher alkylbenzenes are less soluble in water than is benzene. The solubility analogue is complicated by the changing interactions in the pure solute liquid. Such an inversion in partition coefficient has not been observed in RPLC most likely because even when a pure organic mobile phase is used the partition coefficient always prefers the stationary to the mobile phase.

We now turn to the dependence of the free energy terms on the solvent composition. To a first approximation, the cavity term is the product of the solute molar volume and solvent cohesive energy density. The solvent cohesive density increases as the water content increases. The so called "hydrophobic effect"[30] which is generally attributed to an entropic endoergic term due to the reinforcement of the structure of solvent molecules about the solute is very significant for a highly structured solvent such as water[30]. This effect becomes greater as the water content in the mixture increases. Thus the cavity term increases with water content. Such trends are observed in Fig. 7. In addition, the solution process becomes less favorable as the water content increases due to the effect of the cavity term (see Fig. 6).

The dependence of the interaction free energy on solvent composition (Fig. 8) is weaker than the other free energy terms. The strength of the solute–solvent interaction seems to increase slightly with water content. Dispersive interaction should be independent of solvent polarity. Aromatic compounds are weak hydrogen bond accepting bases (Kamlet–Taft basicity is 0.13). Consequently solute–solvent interaction should become stronger as the solvent hydrogen bond donating acidity increases. The solvent dipole–solute-induced dipole interaction should increase as the solvent polarity increases by addition of water. Nevertheless dispersion interactions are generally the major term and the change in the interaction energy with increase in water content is relatively small.

The above arguments can be explored further by examining the dependence of the interaction free energy per CH_2 group on the solvent composition. The interaction free energy of a CH_2 group with the solvent is equivalent to the slope of a plot of ΔG_{int} vs. solute carbon number. Benzene was excluded from the slope calculation because it is the first element of the homologous series and did not fall on the line. The intercept of such a plot (at zero carbon number) also has a significant chemical meaning. If an aromatic CH unit were equivalent to an aliphatic CH_2 unit (or CH_3 unit), then the intercept should be zero. When the intercept is not zero it is a measure of the difference in interaction of an aliphatic CH_2 group and an aromatic CH group with the solvent. The regression results for correlation of ΔG_{int} vs. solute carbon number are assembled in Table VI.

The trends in intercepts are consistent with chemical intuition but as discussed below the slopes are not. The interaction of an aromatic CH unit with the solvent will be greater than that of an aliphatic CH_2 unit due to the hydrogen bond accepting basicity of the aromatic ring as well as its enhanced polarizability. These effects will be reflected in the intercept of the plot of ΔG_{int} vs. solute carbon number. The intercept becomes more exoergic (negative) as the water content increases (Table VI). The intercept values all fall within a narrow range except for a few compositions near the pure organic solvent.

Based on the slopes reported in Table VI, the interaction of an aliphatic CH_2

TABLE VI

THE REGRESSION RESULTS OF ΔG_{int} VS. SOLUTE CARBON NUMBER

Benzene data were excluded in the regression.

System	φ	Intercept ± S.D. (kcal/mol)	Slope ± S.D. (kcal/mol)	Average residual in ΔG_{int}	Correlation coefficient
Methanol–water	0.3	−10.86 ± 0.06	−0.954 ± 0.007	0.015	0.9999
	0.4	−10.48 ± 0.05	−0.929 ± 0.006	0.013	0.9999
	0.5	−10.11 ± 0.04	−0.931 ± 0.005	0.012	0.9999
	0.6	−9.764 + 0.04	−0.945 ± 0.005	0.013	0.9999
	0.7	−9.430 ± 0.05	−0.962 ± 0.005	0.012	0.9999
	0.8	−8.912 ± 0.05	−0.980 + 0.006	0.014	0.9999
	0.9	−8.816 ± 0.06	−1.002 ± 0.008	0.017	0.9999
	1.0	−8.544 ± 0.08	−1.018 ± 0.009	0.020	0.9999
Acetonitrile–water	0.3	−10.44 ± 0.13	−0.943 ± 0.015	0.034	0.9997
	0.4	−9.932 ± 0.17	−0.975 ± 0.017	0.044	0.9996
	0.5	−9.483 ± 0.18	−1.017 ± 0.021	0.047	0.9996
	0.6	−9.065 ± 0.18	−1.047 ± 0.021	0.046	0.9996
	0.7	−8.636 ± 0.16	−1.071 ± 0.019	0.042	0.9997
	0.8	−8.167 ± 0.14	−1.091 ± 0.016	0.037	0.9998
	0.9	−7.631 ± 0.13	−1.111 ± 0.015	0.033	0.9998
	1.0	−7.040 ± 0.14	−1.126 ± 0.016	0.036	0.9998
Isopropanol–water	0.3	−10.25 ± 0.20	−0.822 ± 0.024	0.053	0.9992
	0.4	−9.866 ± 0.18	−0.905 ± 0.021	0.048	0.9995
	0.5	−9.641 ± 0.17	−0.962 ± 0.020	0.045	0.9996
	0.6	−9.505 ± 0.17	−0.996 ± 0.020	0.045	0.9996
	0.7	−9.403 ± 0.18	−1.010 ± 0.021	0.046	0.9996
	0.8	−9.265 ± 0.18	−1.018 ± 0.021	0.047	0.9996
	0.9	−9.025 ± 0.18	−1.035 ± 0.021	0.046	0.9996
	1.0	−8.632 ± 0.16	−1.072 ± 0.019	0.042	0.9997
Tetrahydrofuran–water	0.3	−9.746 ± 0.18	−1.025 ± 0.022	0.048	0.9996
	0.4	−9.234 ± 0.19	−1.092 ± 0.026	0.051	0.9996
	0.5	−8.785 ± 0.20	−1.137 ± 0.023	0.052	0.9996
	0.6	−8.326 ± 0.20	−1.169 ± 0.024	0.053	0.9996
	0.7	−7.804 ± 0.20	−1.190 ± 0.024	0.053	0.9996
	0.8	−7.151 ± 0.20	−1.210 ± 0.023	0.052	0.9996
	0.9	−6.303 ± 0.20	−1.234 ± 0.023	0.051	0.9997
	1.0	−5.264 ± 0.19	−1.257 ± 0.022	0.050	0.9997

group with the solvent, in contrast to an aromatic carbon, becomes more exoergic as the organic cosolvent content increases. This contradicts general chemical intuition. The solvent dipole–solute-induced dipole interaction will be greater for the more polar solvents and the slope of a plot of ΔG_{int} vs. solute carbon number should become less exoergic as the volume fraction of organic component in the solvent increases. This inconsistency can be attributed to several factors. First the above thermodynamic arguments are based on an enthalpic treatment of the process. Entropic treatments of the process are not possible at this time. It should be noted that an entropic treatment may affect the above arguments. Clearly the SRMR model of the cavity term is

imperfect as are our assumptions in extending it to mixed solvents. It should be noted, however, that the slope values are in all cases exoergic and fall within a narrow range.

We conclude that the SRMR method give qualitatively, but not quantitatively, reasonable results for hydro–organic solvent systems.

UNIFAC-calculated activity coefficients

UNIFAC is one of the most powerful and widely used methods for predicting activity coefficients[3,31]. It combines the UNIQUAC model and the ASOG concept. UNIQUAC is an approximate model of liquid mixtures developed by applying Guggenheim's[32] quasi-chemical lattice model of liquid mixtures through the use of local area fraction as the main concentration variable. The ASOG approach is based on the idea that a solution can be viewed as a mixture of independent functional groups of all the components of the solution. In UNIFAC the natural logarithm of the activity coefficient is taken as the sum of a combinatorial part related to volume and area differences and a residual term due to differences in energies of interaction.

Activity coefficients calculated by the UNIFAC method[31] in the solvents reported here differ markedly from the observed values. The experimental (open symbols) and calculated (solid symbols) values as a function of volume fraction of organic cosolvent are compared in Fig. 11 for a typical solute (ethylbenzene).
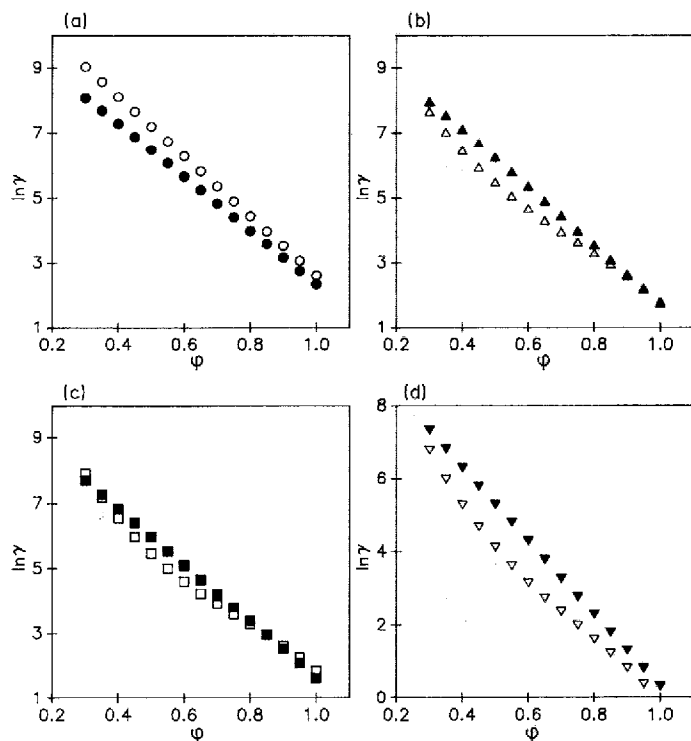

Fig. 11. Comparison of experimental and UNIFAC-calculated activity coefficients. Solute: ethylbenzene. Open symbols: experimental; solid symbols: UNIFAC. (a) Methanol–water system; (b) acetonitrile–water system; (c) isopropanol–water system; (d) tetrahydrofuran–water system.

Examination of Fig. 11 leads to the following observations: (1) the difference between the experimental and UNIFAC calculated values is large. On the natural logarithm scale the error can be as large as 1.5 units. The UNIFAC based activity coefficients are either underestimated by up to 80% or overestimated by up to 200%; (2) the UNIFAC based ln γ^{∞} values are linear with the volume fraction of the organic component (φ), while the experimental ln γ^{∞} values are linear with φ only for methanol–water system; (3) the UNIFAC based activity coefficients are exclusively underestimated for the water system, overestimated for tetrahydrofuran–water system, and overestimated for the acetonitrile–water and isopropanol–water systems in the middle part of solvent composition; (4) agreement is overall best in the pure organic solvents.

The difference between the experimental ln γ^{∞} and the UNIFAC-based ln γ^{∞} was calculated by subtracting the latter from the former. The dependences of this deviation upon solvent composition and solute size are both shown in Fig. 12. The deviation increases with solvent water content and with solute carbon number for the methanol–water system. On the other hand a very different trend is observed for the acetonitrile–water, isopropanol–water, and tetrahydrofuran–water systems (Fig. 12). The variation in Δ ln γ^{∞} for these solvent systems is due to the fact that the UNIFAC-based ln γ^{∞} is linear with φ but the experimental ln γ^{∞} is curved with φ.
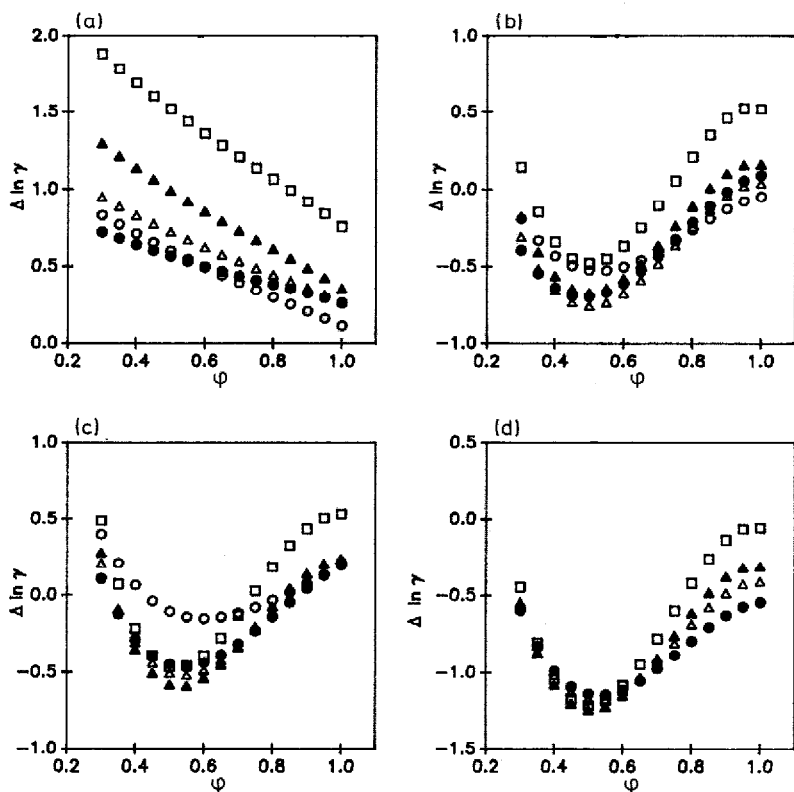

Fig. 12. The difference between the experimental and UNIFAC-based ln γ^{∞} vs. φ. Symbols: $\bigcirc$ = benzene; $\bullet$ = toluene; $\triangle$ = ethylbenzene; $\blacktriangle$ = n-propylbenzene; $\square$ = n-butylbenzene. (a) Methanol–water system; (b) acetonitrile–water system; (c) isopropanol–water system; (d) tetrahydrofuran–water system.

Larger deviations are observed for the methanol–water and tetrahydrofuran–water systems. The modified UNIFAC model[6] was also examined. The differences between the experimental ln γ^∞ and the modified UNIFAC-based ln γ^∞ are given in Fig. 13. With the modified UNIFAC, the predictions at low water content are somewhat improved, but the results at high water content are worsened.

The general failure of the UNIFAC model for predicting activity coefficients of non-polar solutes in aqueous solvents can be attributed to many factors. Most of those have already been described in the literature. The relevant ones are summarized below.

Systems containing water are difficult to describe by either UNIFAC or the modified UNIFAC methods due to the very large non-idealities present[6]. Most published work has centered on vapor–liquid equilibria and hence the interaction parameters are based primarily on experimental data for vapor–liquid equilibria. It may be risky to extend the application of the methods to other areas without adjusting the parameters[4]. Some of the water interaction parameters used in UNIFAC were based on liquid–liquid equilibrium data[1]. The accuracy of UNIFAC improves with an
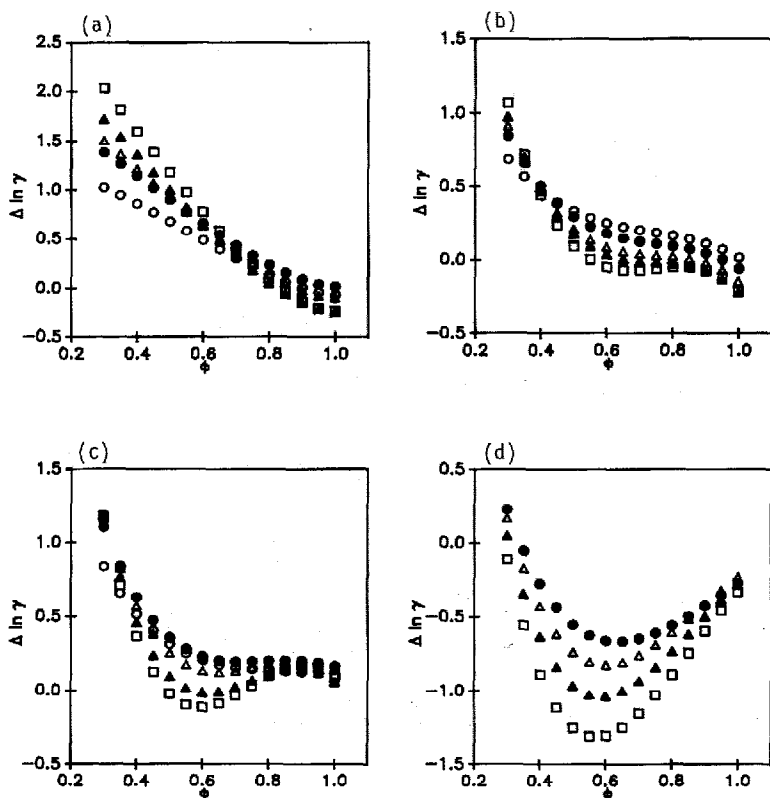

Fig. 13. The difference between the experimental and modified UNIFAC-based ln γ^∞ vs. φ. Symbols: $\bigcirc$ = benzene; $\bullet$ = toluene; $\triangle$ = ethylbenzene; $\blacktriangle$ = n-propylbenzene; $\square$ = n-butylbenzene. (a) Methanol–water system; (b) acetonitrile–water system; (c) isopropanol–water system; (d) tetrahydrofuran–water system.

TABLE VII

ACTIVITY COEFFICIENTS OF THE ALKYLBENZENES IN MIXTURES OF WATER WITH METHANOL, ACETONITRILE, ISOPROPANOL AND TETRAHYDROFURAN AT 25°C

φ = Volume fraction of organic cosolvent, B = benzene, T = toluene, EB = ethylbenzene, PB = n-propylbenzene, BB = n-propylbenzene, C = cumene, TB = tert.-butylbenzene.

System	Activity coefficients ± S.D.						
φ	B	T	EB	PB	BB	C	TB
Methanol–water							
0.3	—	—	—	—	—	—	—
0.35	663	1820	5240	17 200	68 800	12 700	28 000
0.4	495	1270	3420	10 600	39 200	7290	16 600
0.45	349 ± 14	853 ± 23	2140 ± 33	6300 ± 59	22 500 ± 750	4780 ± 69	9670 ± 76
0.5	247 ± 13	568 ± 28	1360 ± 54	3670 ± 140	12 200 ± 30	2820 ± 117	5480 ± 211
0.55	174 ± 9.9	379 ± 22	852 ± 45	2140 ± 107	6650 ± 120	1670 ± 89	3120 ± 165
0.6	119 ± 6.8	250 ± 11	537 ± 32	1220 ± 83	3620 ± 72	1010 ± 45	1790 ± 98
0.65	84 ± 4.7	167 ± 7	338 ± 20	718 ± 42	1990 ± 35	604 ± 28	999 ± 55
0.7	59 ± 2.8	112 ± 5	214 ± 12	425 ± 19	1100 ± 21	362 ± 18	578 ± 22
0.75	41 ± 1.8	75 ± 2.5	136 ± 6	252 ± 7	612 ± 20	218 ± 12	335 ± 6
0.8	29.0 ± 1.1	50 ± 1.6	86 ± 4	150 ± 1.2	341 ± 19	132 ± 9.9	195 ± 2
0.85	20.3 ± 0.6	33 ± 1.0	54 ± 2	89 ± 1.3	197 ± 16	82 ± 7.8	116 ± 0.2
0.9	14.2 ± 0.3	22 ± 0.8	34 ± 0.9	54.5 ± 0.6	120	50 ± 5.0	69 ± 0.6
0.95	9.9 ± 0.2	15.0 ± 0.6	21.8 ± 0.6	—	70	33	—
1.0	7.0 ± 0.1	10.1 ± 0.5	13.9 ± 0.5	17.3 ± 0.3	24.8 ± 0.9	15.7 ± 0.2	19.1 ± 0.2
Acetonitrile–water							
0.3	324	820	2160	6200	20 300	4690	9200
0.35	199	460	1090	2840	8300	2190	4030
0.4	132 ± 1.1	280 ± 3	622 ± 9	1500 ± 27	4120 ± 16	1170 ± 8	2060 ± 17
0.45	89.7 ± 0.1	182 ± 4	381 ± 10	868 ± 18	2250 ± 31	685 ± 11	1160 ± 23
0.5	62.8 ± 0.1	123 ± 3	246 ± 8	535 ± 9	1310 ± 29	424 ± 8	695 ± 16
0.55	44.8 ± 0.3	85 ± 2	164 ± 4.9	344 ± 2	806 ± 18	273 ± 5	436 ± 8
0.6	32.4 ± 0.6	60 ± 1.4	111 ± 2.8	228 ± 2	511 ± 9	181 ± 2	282 ± 6
0.65	23.5 ± 0.6	42.4 ± 1.3	75.8 ± 2.3	153 ± 4	330 ± 4	119 ± 4	182 ± 6
0.7	17.4 ± 0.6	30.7 ± 0.8	53.3 ± 1.3	101 ± 0.8	219 ± 3	82 ± 2	123 ± 2
0.75	12.9 ± 0.6	22.3 ± 0.5	37.7 ± 0.8	68.5 ± 1.3	147 ± 4	57 ± 1	84 ± 1.5
0.8	9.6 ± 0.6	16.3 ± 0.4	26.9 ± 0.5	46.9 ± 1.3	99 ± 4	39.6 ± 1.0	57.6 ± 1.4
0.85	7.5 ± 0.1	12.0 ± 0.5	19.2 ± 0.4	31.6	65	27.8 ± 1.3	40.0 ± 2.0
0.9	5.6 ± 0.1	8.8 ± 0.4	13.9 ± 0.5	21.9	44	19.6 ± 1.2	27.6 ± 2.0
0.95	4.1	6.3	9.6 ± 0.4	15.3	29	13.0	17.8
1.0	2.9 ± 0.2	4.3 ± 0.3	5.6 ± 0.3	7.8	11.1	6.9	8.2

Isopropanol–water

	1	2	3	4	5	6	7
0.3	534 ± 8	1220 ± 11	2900 ± 10	6940 ± 2	19 400 ± 15	5660 ± 14	10 600 ± 23
0.35	299 ± 4	606 ± 4	1240 ± 6	2730 ± 16	6670 ± 30	2220 ± 20	3710 ± 20
0.4	193 ± 2	352 ± 2	640 ± 2	1270 ± 16	2840 ± 30	1060 ± 14	1670 ± 13
0.45	127 ± 0.9	216 ± 1.4	377 ± 1.4	680 ± 11	1430 ± 22	579 ± 9	878 ± 8
0.5	88 ± 0.6	141 ± 0.9	234 ± 0.5	394 ± 7	796 ± 15	341 ± 6	505 ± 4
0.55	62.1 ± 0.3	95.1 ± 0.6	153 ± 0.4	243 ± 4	476 ± 8	214 ± 2	310 ± 2
0.6	44.8 ± 0.2	66.2 ± 0.6	103 ± 0.3	157 ± 2.4	300 ± 5	139 ± 2	199 ± 1.4
0.65	32.7 ± 0.3	47.0 ± 0.5	71.1 ± 0.1	108 ± 0.9	200 ± 3	95 ± 0.7	133 ± 0.5
0.7	24.4 ± 0.2	34.1 ± 0.3	50.4 ± 0.3	74.7 ± 0.6	136 ± 1.3	66 ± 0.2	91.1 ± 0.3
0.75	18.3 ± 0.1	24.9 ± 0.2	36.0 ± 0.3	52.7 ± 1.4	94	46.8 ± 0.7	63.3 ± 1.0
0.8	13.7 ± 0.1	18.3 ± 0.3	26.0 ± 0.5	37.8	64.6	33.4 ± 1.1	44.5
0.85	10.4 ± 0.1	13.7 ± 0.3	18.8 ± 0.6	26.9	43	23.8 ± 0.1	31.2
0.9	7.9 ± 0.1	10.2 ± 0.3	13.6 ± 0.2	18.0	30	17.1	21.1
0.95	6.0	7.6 ± 0.2	9.9	12.6	20.5	11.4	14.6
1.0	4.5	5.3	6.2	7.0	8.5	7.0	7.3

Tetrahydrofuran–water

	1	2	3	4	5	6	7
0.3	—	—	—	—	—	—	—
0.35	—	—	—	—	—	—	—
0.4	—	112 ± 4	197 ± 7	349 ± 21	700 ± 41	300 ± 16	446 ± 30
0.45	—	65 ± 2	107 ± 3	178 ± 9	331 ± 18	155 ± 6	220 ± 11
0.5	—	40.0 ± 0.8	62.1 ± 1.8	98.2 ± 4.0	171 ± 8	87 ± 2	119 ± 5
0.55	—	25.5 ± 0.4	38.2 ± 0.9	57.8 ± 1.9	95.1 ± 3.7	51.3 ± 1.1	68.3 ± 2.3
0.6	—	16.8 ± 0.2	24.3 ± 0.5	35.4 ± 0.9	55.8 ± 1.6	31.7 ± 0.5	41.2 ± 1.1
0.65	—	11.3 ± 0.1	15.9 ± 0.2	22.5 ± 0.4	36.0 ± 3.1	20.2 ± 0.2	25.9 ± 0.7
0.7	—	7.8 ± 0.1	10.7 ± 0.2	14.6 ± 0.4	22.1 ± 0.7	13.2 ± 0.2	16.6 ± 0.4
0.75	—	5.41 ± 0.04	7.23 ± 0.13	9.61 ± 0.2	14.1 ± 0.2	8.70 ± 0.1	10.7 ± 0.2
0.8	—	3.78 ± 0.03	4.95 ± 0.01	6.36 ± 0.04	9.3 ± 0.4	5.78 ± 0.1	7.03 ± 0.06
0.85	—	2.64 ± 0.05	3.39 ± 0.06	4.22 ± 0.09	5.85	3.85 ± 0.08	4.61 ± 0.12
0.9	—	1.86 ± 0.08	2.33 ± 0.09	2.81 ± 0.18	3.96	2.58 ± 0.14	3.05 ± 0.17
0.95	—	1.25	1.52	1.73	—	1.62	—
1.0	—	0.84	0.90	0.91	0.90	0.88	0.87

increase in the number of defined groups[3]. The number of distinct groups should be kept small but not so small as to neglect significant effects of molecular structure on physical properties[33]. When the parameters are based on scarce or poor data, much larger average deviations should be expected[33]. If UNIFAC parameters were developed based on only activity coefficients at infinite dilution, instead of including many data at finite concentration, UNIFAC should be able to predict better γ^{∞} values[33]. It is seen that the largest deviations occur in alcohol- and water-containing systems[5]. UNIFAC is not able to handle polar molecules with cyclic backbones[34].

Based on the above arguments and the results of this study we suspect that the UNIFAC parameters for aqueous systems were based on poor data. This argument is supported by recent work[35] in which a new set of interaction parameters were computed based on only infinite dilution activity coefficient data. Unfortunately water–aromatic CH group interaction parameters were not reported and thus could not be tested in this study. A separate set of UNIFAC parameters might be necessary for extremely non-ideal systems such as non-polar solutes in very polar solvents. The data reported here should be useful for this purpose. For example "satellite" UNIQUAC/UNIFAC models with their own parameter tables have been useful for improving UNIFAC predicts for the systems containing ions, polymers and gases[5].

Different group interaction parameters may be necessary for CH_2 and CH_3 groups because the deviation between the experimental and UNIFAC data greatly increases when a CH_2 group is added (compare propylbenzene to butylbenzene, Fig. 2). In the UNIFAC model CH_2 and CH_3 units are defined as having the same interaction parameters. Tetrahydrofuran may also have to be defined as a separate group. As stated in ref. 34, UNIFAC is incapable of handling polar molecules with cyclic backbones.

APPENDIX

Activity coefficients
It must be noted that the values in Table VII are not measured data. Because it was impossible to work at the same set of volume fractions in the many series of runs carried out in this study, we were not able to directly compare the precision of measurement on the raw data. Instead, we fit the measured values to the volume fractions using a Pade approximant of the form given below:

$$\ln \gamma^{\infty} = \frac{a + b\varphi + c\varphi^2}{1 + d\varphi}$$

This approach was taken to minimize oscillations in the fitting function which is a common problem with high order polynomial fits of the type shown in eqn. 1. Once a fit was obtained, it was used to interpolate, never to extrapolate, to the volume fractions given in the table. The numbers adjacent to the activity coefficient are the computed standard deviations between several series of runs. Where no standard deviation is shown, the data for that volume fraction were only collected once. In general, data were collected at volume fraction increments of considerably less than 0.05 and each result is typically based on at least three separate runs at different concentrations of the solutes.

REFERENCES

1 E. H. Slaats, J. C. Kraak, W. J. T. Brugman and H. Poppe, *J. Chromatogr.*, 149 (1978) 225.
2 M. Schantz, B. N. Barman and D. E. Martire, *J. Res. Natl. Bur. Stand. (U.S.)*, 93 (1988) 161.
3 D. S. Abrams and J. M. Prausnitz, *AIChE J.*, 21 (1975) 116.
4 E. L. Derr and C. H. Deal, *I. Chem. E. Symp. Ser.*, No. 32 (1969) 37.
5 A. Fredenslund and P. Rasmussen, *Fluid Phase Equilib.*, 24 (1985) 115.
6 B. L. Larsen, P. Rasmussen and A. Fredenslund, *Ind. Eng. Chem. Res.*, 26 (1987) 2274.
7 E. E. Tucker, E. H. Lane and S. D. Christian, *J. Solution Chem.*, 10 (1981) 1.
8 J. H. Park, *Ph.D. Thesis*, University of Minnesota, Minnesota, 1988.
9 J. H. Park, A. Husam, P. Couasnon, D. Fritz and P. W. Carr, *Anal. Chem.*, 59 (1987) 1970.
10 W. J. Cheong and P. W. Carr, *J. Chromatogr.*, 499 (1990) 373.
11 A. Husam and P. W. Carr, *Anal. Chem.*, 57 (1985) 793.
12 J. A. Riddick and W. B. Burger, *Organic Solvents —Physical Properties and Methods of Purification*, Wiley-Interscience, New York, 1970.
13 A. Ben-Naim, *Hydrophobic Interactions*, Plenum Press, New York, 1980.
14 A. Ben-Naim and Y. Marcus, *J. Chem. Phys.*, 80 (1984) 4438.
15 A. Ben-Naim, *J. Phys. Chem.*, 82 (1978) 792.
16 J. H. Hildebrand, J. M. Prausnitz and R. L. Scott, *Regular and Related Solutions*, Van Nostrand, New York, 1970.
17 K. Shinoda, *Principles of Solutions and Solubility*, Marcel Dekker, New York, 1978.
18 R. A. Pierotti, *J. Phys. Chem.*, 67 (1963) 1840.
19 R. A. Pierotti, *Chem. Rev.*, 76 (1976) 717.
20 O. Sinanoglu, in B. Pullman (Editor), *Molecular Association in Biology*, Academic Press, New York, 1968, p. 427.
21 T. Halicioglu and O. Sinanoglu, *Ann. N.Y. Acad. Sci.*, 158 (1969) 308.
22 J. J. Moura Ramos, J. Reiss and M. H. Abraham, *Can. J. Chem.*, 57 (1979) 500.
23 J. Reiss, personal communication, 1988.
24 W. J. Cheong and P. W. Carr, *J. Liq. Chromatogr.*, 10 (1987) 561.
25 B. L. Karger, L. R. Snyder and Cs. Horváth, *An Introduction to Separation Science*, Wiley, New York, 1973.
26 J. H. Hildebrand and R. I. Scott, *The Solubility of Non-Electrolytes*, Dover, New York, 3rd ed., 1964.
27 S. C. Rutan, P. W. Carr, W. J. Cheong, J. H. Park and L. R. Snyder, *J. Chromatogr.*, 463 (1989) 21.
28 M. H. Abraham, *J. Chem. Soc. Faraday Trans. I*, 80 (1984) 153.
29 M. M. Schantz and D. E. Martire, *J. Chromatogr.*, 35 (1987) 391.
30 C. Tanford, *The Hydrophobic Effect: Formation of Micelles and Biological Membranes*, Wiley, New York, 1973.
31 J. Gmehling, P. Rasmussen and A. Fredenslund, *Ind. Eng. Chem. Process Des. Dev.*, 21 (1982) 118.
32 E. A. Guggenheim, *Mixtures*, Clarendon Press, Oxford, 1952.
33 P. Rasmussen and A. Fredenslund, *Separ. Purif. Methods*, 7 (1978) 147.
34 E. R. Thomas and C. A. Eckert, *Ind. Eng. Chem. Process Des. Dev.*, 23 (1984) 194.
35 J. C. Bastos, M. E. Soares and A. G. Medina, *Ind. Eng. Chem. Res.*, 27 (1988) 1269.